

Counterion Effect on CO/Styrene Copolymerization Catalyzed by Cationic Palladium(II) Organometallic Complexes: An Interionic Structural and Dynamic Investigation Based on NMR Spectroscopy[§]

Alceo Macchioni,* Gianfranco Bellachioma, Giuseppe Cardaci,
Monia Travaglia, and Cristiano Zuccaccia

Dipartimento di Chimica, Università di Perugia, Via Elce di Sotto, 8-06123 Perugia, Italy

Barbara Milani, Gianni Corso, Ennio Zangrando, and Giovanni Mestroni

*Dipartimento di Scienze Chimiche, Università di Trieste, Via Licio Giorgieri,
1-34127 Trieste, Italy*

Carla Carfagna and Mauro Formica

*Istituto di Scienze Chimiche, Università di Urbino, Piazza Rinascimento,
6-61029 Urbino, Italy*

Received May 18, 1999

Complexes $[\text{Pd}(\eta^1, \eta^2\text{-C}_8\text{H}_{12}\text{OMe})\text{bipy}]^+\text{X}^-$ (**2a–f**) (where $\text{X} = \text{BPh}_4^-$ (**a**), CF_3SO_3^- (**b**), BF_4^- (**c**), PF_6^- (**d**), SbF_6^- (**e**), and $\text{B}(3,5\text{-(CF}_3)_2\text{C}_6\text{H}_3)_4^-$ (**f**); bipy = 2,2'-bipyridine; $\text{C}_8\text{H}_{12}\text{OMe}$ = cyclooctenylmethoxy group) were synthesized by the reaction of the dimer $[\text{Pd}(\eta^1, \eta^2\text{-C}_8\text{H}_{12}\text{OMe})\text{Cl}]_2$ (**1**) with the bipy ligand in methanol containing Y^+X^- salts. They were characterized in solution by multinuclear and multidimensional NMR spectroscopy. The solid-state structure of complex **2d** was obtained by X-ray single-crystal investigation. The catalytic activity of complexes **2** toward CO/styrene copolymerization in methylene chloride was tested and related to the type of counterion. The order of the catalytic activity of complexes **2a–f** is the following: $\text{BPh}_4^- \ll \text{CF}_3\text{SO}_3^- < \text{BF}_4^- < \text{PF}_6^- < \text{SbF}_6^- < \text{B}(3,5\text{-(CF}_3)_2\text{C}_6\text{H}_3)_4^-$. If the copolymerization reactions are carried out in the presence of an excess of the bipy ligand, the anion effect is less important and the order is the following: $\text{BPh}_4^- \ll \text{CF}_3\text{SO}_3^- < \text{BF}_4^- \approx \text{B}(3,5\text{-(CF}_3)_2\text{C}_6\text{H}_3)_4^- \approx \text{PF}_6^- \approx \text{SbF}_6^-$. The interionic structure of all complexes was investigated in CD_2Cl_2 at room and low temperature by $^{19}\text{F}\{^1\text{H}\}$ HOESY and ^1H NOESY NMR spectroscopies. In solution, the counterions are located above or below the bipy ligand shifted toward the pyridine ring trans to the Pd–C σ bond, while in the crystal structure of **2d**, they are settled sideways to the cationic moiety. The best anion in catalysis is the least strong coordinating one that shows the weakest interionic contacts in the $^{19}\text{F}\{^1\text{H}\}$ HOESY or ^1H NOESY NMR spectra. The dynamic process that exchanges the two pyridyl rings was investigated by variable-temperature NMR spectroscopy in CD_2Cl_2 . The activation parameters were determined. ΔG^\ddagger_{298} values range from 54 to 58 kJ/mol. The negative values of ΔS^\ddagger (–58/–108 J K^{–1} mol^{–1}), for all compounds, with the exception of **2f**, suggest an associative mechanism.

Introduction

During the past few years, some of us have been involved in the investigation of the interionic solution structure of charged organometallic complexes by NMR spectroscopy.¹ The principal aim of our studies has been addressed to determine the relative cation–anion position in solution and, in particular, in solvents where intimate ion-pairs are mainly present. This can be done

by detecting the interionic dipolar interaction between the NMR-active nuclei of the organometallic fragment and those belonging to its counterion. Our previous studies on model compounds, based on NOESY and HOESY NMR spectroscopies, have demonstrated that in methylene chloride solution the counterion not only prefers to stay in a specific position^{1,2} but also has a preferential orientation when it is unsymmetric.³ This

[§] Dedicated to the memory of Michelangelo Minciotti.

* To whom correspondence should be addressed.

(1) Bellachioma, G.; Cardaci, G.; Macchioni, A.; Reichenbach, G.; Terenzi, S. *Organometallics* **1996**, *15*, 4349–4351. Macchioni, A.; Bellachioma, G.; Cardaci, G.; Gramlich, V.; Rüegger, H.; Terenzi, S.; Venanzi, L. M. *Organometallics* **1997**, *16*, 2139–2145.

(2) Macchioni, A.; Bellachioma, G.; Cardaci, G.; Cruciani, G.; Foresti, E.; Sabatino, P.; Zuccaccia, C. *Organometallics* **1998**, *17*, 5549–5556. Bellachioma, G.; Cardaci, G.; Gramlich, V.; Macchioni, A.; Valentini, M.; Zuccaccia, C. *Organometallics* **1998**, *17*, 5025–5030.

(3) Zuccaccia, C.; Bellachioma, G.; Cardaci, G.; Macchioni, A. *Organometallics* **1999**, *18*, 1–3.

makes possible the estimation of the average interionic distances³ by measuring the kinetics of NOE buildup.

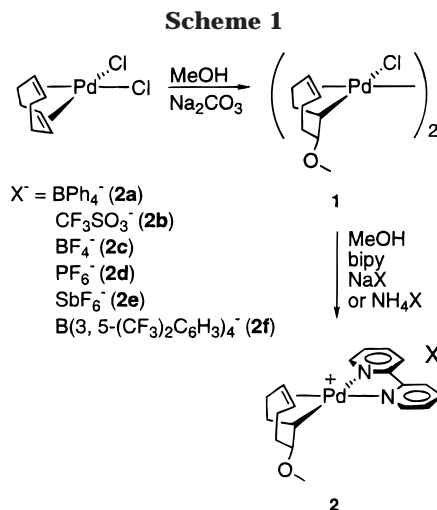
To the best of our knowledge such information about the structure of ion-pairs in solution is very difficult to obtain by other methods. Furthermore, it is very important for homogeneous catalysis. It is in fact well-known from the literature⁴ that several processes, mediated by charged organometallic complexes, are strongly dependent on the nature of the counterion. The possibility of directly observing the anion-cation interactions in solution could lead to a better understanding of the role of the anion in the catalytic processes and to optimizing the choice of the "cation-anion pair".

For this reason we decided to investigate the interionic structure of $[\text{Pd}(\eta^1, \eta^2\text{-C}_8\text{H}_{12}\text{OMe})\text{bipy}]^+\text{X}^-$ ⁵ organometallic complexes because (1) they are active catalysts for CO/styrene copolymerization⁶ in methylene chloride at room temperature and atmospheric pressure and (2) while all the protons are unsymmetrically distributed around palladium, their resonances are well resolved in the ¹H NMR spectrum, which allows the eventual effects of the counterion interactions to be clearly detected.

In this paper, we report the syntheses of complexes $[\text{Pd}(\eta^1, \eta^2\text{-C}_8\text{H}_{12}\text{OMe})\text{bipy}]^+\text{X}^-$ (**2a–f**) (where X = BPh₄[−] (**a**), CF₃SO₃[−] (**b**), BF₄[−] (**c**), PF₆[−] (**d**), SbF₆[−] (**e**), and B(3,5-(CF₃)₂C₆H₃)₄[−] (**f**); bipy = 2,2'-bipyridine; C₈H₁₂-OMe = cyclooctenylmethoxy group), their catalytic activity toward the CO/styrene copolymerization, and the crystal structure of complex **2d**. We also describe the determination of the interionic structure in solution of the complexes by ¹⁹F{¹H} HOESY and ¹H NOESY NMR spectroscopies. Finally, the activation parameters of the dynamic process that averages the two pyridine rings in the ¹H NMR spectra as a function of the counterion nature are presented.

Results and Discussion

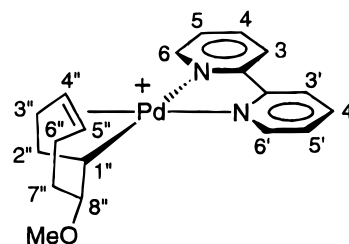
Synthesis. Organometallic complexes were synthesized according to Scheme 1 as reported in the literature.⁵ The first step of the reaction involves a direct exo attack⁷ of MeO[−] on the coordinated cyclooctadiene with the formation of compound **1** as an air-stable, pale yellow solid. Compound **1** reacts in methanol with 2,2'-bipyridine in the presence of NH₄X or NaX (X = BPh₄[−],



CF₃SO₃[−], BF₄[−], PF₆[−], SbF₆[−], and B(3,5-(CF₃)₂C₆H₃)₄[−]), forming complexes **2a–f**, which precipitate from solution. Compounds **2c–e** are stable for several hours in methylene chloride solution at room temperature (≈298 K) under inert atmosphere. Complexes **2b** and **2f** start to transform into unidentified compounds within a few minutes, while **2a** decomposes into Pd metal within a few minutes.

Characterization and Structure. (a) Intramolecular Solution Structure. Complexes **2a–f** were characterized in methylene chloride solution by ¹H, ¹³C, ¹⁹F, and ³¹P NMR spectroscopies.

The olefinic and aliphatic regions of the ¹H NMR spectra do not show any particular features, and the complete assignment is reported in the Experimental Section. On the other hand, the aromatic region of the ¹H NMR spectra at room temperature (304 K) shows only three resonances, and each of them integrates for two protons (for an example see the ¹H NMR spectrum of complex **2c** recorded at 302 K, reported in Figure 3). The resonance relative to the 6–6' couple is apparently missing. A dynamic process that averages the two pyridine rings is present (see below). This makes the four proton pairs equivalent (6–6', 5–5', 4–4', and 3–3', see numeration below). Due to this reason, the aforementioned relative instability of complexes **2a**, **2b**, and **2f** in solution at room temperature, and the need to differentiate all the positions around palladium in order to better localize the counterions (see below), we performed low-temperature NMR experiments.



At 217 K the two pyridine rings are no longer equivalent in all the complexes, and consequently, eight resonances are present in the aromatic region of the ¹H NMR spectra. In Table 1 we report the chemical shifts of these resonances and those of the cyclooctenyl protons that are more sensitive to counterion type at 217 K. A

(a) Chen, Y.-X.; Metz, M. V.; Li, L.; Stern, C. L.; Marks, T. J. *J. Am. Chem. Soc.* **1998**, *120*, 6287–6305. (b) Chen, Y.-X.; Stern, C. L.; Marks, T. J. *J. Am. Chem. Soc.* **1997**, *119*, 2582–2583. (c) Jia, L.; Yang, X.; Stern, C. L.; Marks, T. J. *Organometallics* **1997**, *16*, 842–857. (d) Chen, Y.-X.; Stern, C. L.; Yang, X.; Marks, T. J. *J. Am. Chem. Soc.* **1996**, *118*, 12451–12452. (e) Yang, X.; Stern, C. L.; Marks, T. J. *J. Am. Chem. Soc.* **1994**, *116*, 10015–10031. (f) Johnson, L. K.; Mecking, S.; Brookhart, M. *J. Am. Chem. Soc.* **1996**, *118*, 267–268. (g) Drent, E.; Budzelaar, P. H. M. *Chem. Rev.* **1996**, *96*, 663–681. (h) Milani, B.; Vicentini, L.; Sommazzi, A.; Garbassi, F.; Chiarparin, E.; Zangrando, E.; Mestroni, G. *J. Chem. Soc., Dalton Trans.* **1996**, 3139–3144. (i) Lightfoot, A.; Schnider, O.; Pfaltz, A. *Angew. Chem., Int. Ed. Engl.* **1998**, *37*, 2897–2899.

(5) The synthesis of compounds with the 2,2'-bipyridyl- and 1,10-phenanthroline ligand and with X[−] = PF₆[−] was previously reported: Pietropaolo, G.; Cusmano, F.; Rotondo, E.; Spadaro, A. *J. Organomet. Chem.* **1978**, *155*, 117–122.

(6) Milani, B.; Mestroni, G.; Sommazzi, A.; Garbassi, F. Italian Patent N. MI 95/A 000337, 1995; European Patent N. 96101967.6-2102, 1996.

(7) Hoel, G. R.; Stockland, R. A., Jr.; Anderson, G. K.; Lapido, F. T.; Braddock-Wilking, J.; Rath, N. P.; Mareque-Rivas, J. C. *Organometallics* **1998**, *17*, 1155–1165.

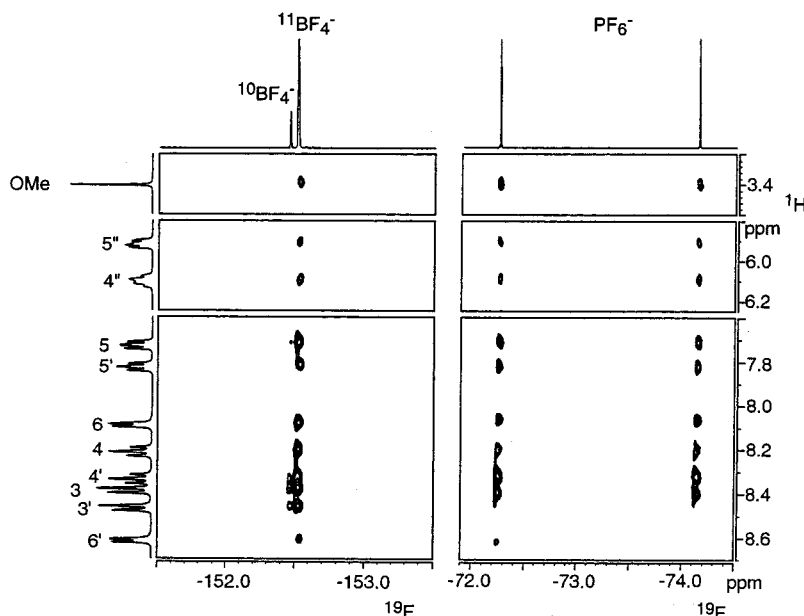


Figure 1. Three sections of the $^{19}\text{F}\{^1\text{H}\}$ HOESY NMR spectra of complexes **2c** and **2d** recorded at 376 MHz in CD_2Cl_2 at 217 K showing that (a) the interionic contacts between the counterions and aromatic protons are stronger than those with aliphatic protons and (b) the interionic contact between $6'$ and the counterion is significantly weaker than the other aromatic contacts.

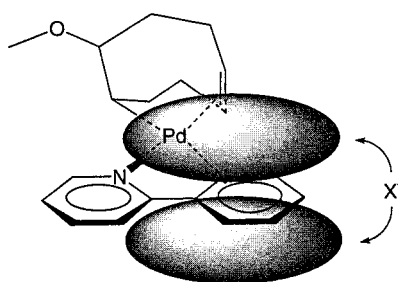


Figure 2. Representation of the interionic structure in solution deduced from interionic NMR investigations. The counterion X^- appear to be localized above or below the bipyridine ligand but shifted toward the pyridine ring trans to the $\text{Pd}-\text{C}$ σ bond, as indicated by the gray cloud.

complete assignment of all the ^1H and ^{13}C resonances has been done for complex **2d** by recording the ^1H COSY, ^1H NOESY, and $^1\text{H}\{^{13}\text{C}\}$ COSY ("standard" and long-range) NMR spectra both at room (304 K) and low (217 K) temperatures. In particular, it is possible to distinguish the pyridine ring that is trans to the $\text{Pd}-\text{C}$ σ bond from that which is trans to the olefinic fragment by detecting the intramolecular contacts between the 6 and $4''-5''$ protons and between the $6'$ protons and the $8''$ and OMe ones, in the ^1H NOESY spectrum.

(b) Solution Interionic Structure. The interionic structure has been investigated by recording (1) the $^{19}\text{F}\{^1\text{H}\}$ HOESY NMR spectra both at 304 K and at 217 K for complexes **2b-d**, (2) the ^1H NOESY NMR spectrum of the **2a** complex only at 217 K, (3) both the $^{19}\text{F}\{^1\text{H}\}$ HOESY and ^1H NOESY NMR spectra at 217 K for **2f**. Complex **2e** could not be studied by $^{19}\text{F}\{^1\text{H}\}$ HOESY NMR spectroscopy due to the presence of ^{121}Sb ($I = 5/2$, natural abundance = 57.25) and ^{123}Sb ($I = 7/2$, natural abundance = 42.75), which afford 14 broad resonances in the fluorine NMR spectrum with eventual interionic interactions that are too disperse to be detected. All the measurements were carried out in CD_2Cl_2 , the solvent used for copolymerization reactions.

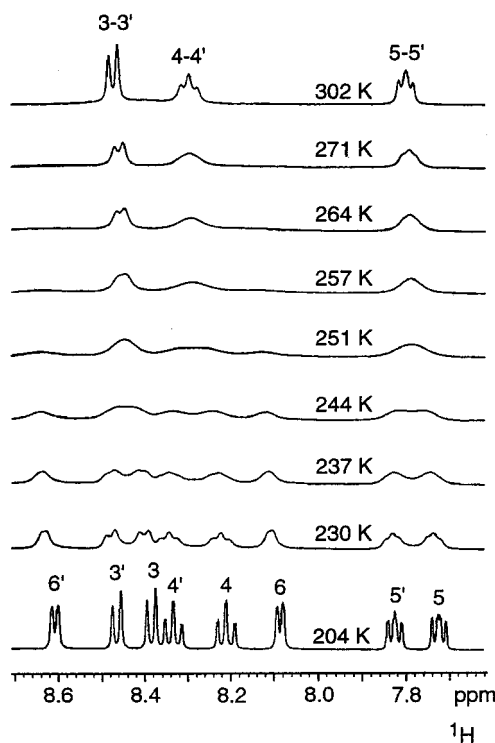


Figure 3. Variable-temperature ^1H NMR spectra of complex **2c** recorded at 400.13 MHz in CD_2Cl_2 showing the passage from slow to fast exchange for $3-3'$, $4-4'$, and $5-5'$ protons. At 302 K the resonances of protons $6-6'$ are so broad that they are apparently missing.

From the literature, it is known that in this solvent analogous complexes are mainly present as intimate ion-pairs.⁸

The $^{19}\text{F}\{^1\text{H}\}$ HOESY NMR spectra recorded at 304 K for complexes **2b-d** show strong interionic interactions

(8) Romeo, R.; Arena, G.; Monsù Scolaro, L.; Plutino, M. R. *Inorg. Chim. Acta* **1995**, *240*, 81-92.

Table 1. Selected ^1H NMR Chemical Shift Values Obtained in CD_2Cl_2 at 217 K for Compounds **2a–f**

	2a	2b	2c	2d	2e	2f
3	7.67	8.45	8.38	8.32	8.31	8.12
3'	7.72	8.52	8.46	8.40	8.39	8.19
4	7.87	8.21	8.21	8.20	8.20	8.07
4'	7.96	8.34	8.33	8.32	8.32	8.18
5	7.40	7.73	7.72	7.72	7.72	7.61
5'	7.61	7.83	7.82	7.82	7.83	7.75
6	7.62	8.11	8.09	8.06	8.07	7.99
6'	8.52	8.62	8.61	8.60	8.62	8.61
1''	2.92	2.96	2.97	2.96	2.97	2.97
4''	5.79	6.12	6.11	6.09	6.09	6.05
5''	5.69	5.92	5.91	5.91	5.91	5.87
8''	3.66	3.68	3.67	3.67	3.68	3.66
OMe	3.41	3.40	3.40	3.40	3.40	3.39

between the fluorine atoms of the counterion and all the aromatic protons. Whereas there are weak contacts with protons that are close to palladium (4'', 5'', 1'', 8'', and OMe), are no interactions with the other protons of the $\eta^1, \eta^2\text{-C}_8\text{H}_{12}\text{OMe}$ ligand (2'', 3'', 6'', and 7''). The above observations indicate that the counterion is localized above or below the coordination plane in all three complexes and is shifted toward the bipyridine ligand. The strength of the contacts follow the order **2c** > **2d** > **2b**, but it must be considered that, while BF_4^- and PF_6^- have the fluorine atoms homogeneously distributed around the negative charge, in CF_3SO_3^- , the fluorines point away from it. This means that the distance between the fluorine atoms and the protons of the charged organometallic moiety is structurally longer and, consequently, the interionic contacts are weaker than those for BF_4^- and PF_6^- .

The $^{19}\text{F}\{^1\text{H}\}$ HOESY and ^1H NOESY NMR spectra recorded at 217 K for complexes **2b–d** and **2a**, respectively, again show strong interionic contacts between the atoms of the counterions and the aromatic protons and weak contacts with protons 4'', 5'', 1'', 8'', and OMe. At this temperature, it is possible to distinguish the protons belonging to the two different pyridine rings, and it is interesting to note that the counterion interacts preferentially with the ring that is trans to the η^1 -arm of the cyclooctenyl derived ligand (see Figure 1) in complexes **2b–d**. Therefore the low-temperature experiments not only confirm that the counterion is localized both above and below the bipyridine ligand but also indicate that it is shifted toward the pyridine ring that is trans to the Pd–C single bond (see Figure 2). It is impossible to understand if this is also true for complex **2a** because, in this case, the dynamic process that exchanges the two pyridine rings is fast on the longitudinal relaxation time scale and the cross-peaks between the protons of the counterion and those of a proton pair that are exchanging have the same intensity.⁹

Confirmation of the interionic structure depicted in Figure 2 has been derived from the analysis of the chemical shifts of the aromatic protons reported in Table 1. The shifts related to complexes **2a** and **2f** are particularly indicative because the proximity of the aromatic rings of the counterion to the protons of the cationic fragment are indicated by a shielding effect.¹⁰

(9) Neuhaus, D.; Williamson, M. *The Nuclear Overhauser Effect in Structural and Conformational Analysis*; VCH Publishers: New York, 1989; pp 141–181.

Table 2. Activation Energy Data for Complexes **2a–f** in CD_2Cl_2

	ΔH^\ddagger (kJ/mol)	ΔS^\ddagger (J/(mol K))	ΔG^\ddagger_{298} (kJ/mol)
2a	26 ± 1	−108 ± 5	58 ± 3
2b	38 ± 2	−58 ± 8	55 ± 5
2c	36 ± 1	−59 ± 4	54 ± 2
2d	33 ± 1	−86 ± 3	59 ± 2
2e	35 ± 1	−83 ± 4	60 ± 2
2f	61 ± 3	13 ± 10	57 ± 6

The effect is more marked for compound **2a** because of a higher electron density on the aromatic rings. Indeed the protons that exhibit the strongest interionic contacts are those that are more shielded with respect to the same protons of complex **2b** ($\Delta\delta$ up to 0.80 ppm for 3 and 3'). The different behavior of protons 6 and 6' that are shielded by 0.49 and 0.10 ppm, respectively, is significant and in perfect agreement with the findings of the interionic structure that indicate a shift of the counterion toward the pyridine ring that is trans to the Pd–C single bond.

The ^1H NOESY NMR spectrum for complex **2f** recorded at 217 K does not show any interionic contact, while the $^{19}\text{F}\{^1\text{H}\}$ HOESY NMR spectrum shows only a weak contact between the fluorine atoms of the counterion and the bipy proton in position 4. This is not surprising because $\text{B}(3,5\text{-(CF}_3)_2\text{C}_6\text{H}_3)_4^-$ is such a weak coordinating anion¹¹ that its salts can give nonintimate ion pairs even in methylene chloride.¹² In any case, it is interesting to note that the only weak interionic contact that we observe in the $^{19}\text{F}\{^1\text{H}\}$ HOESY NMR spectrum is with an aromatic proton. This means that the interionic structure of the few intimate ion pairs of complex **2f** is probably the same as that of the other complexes.

(c) Dynamic Behavior of Complexes 2a–f. The aforementioned dynamic process that equilibrates the environment of the two pyridine rings was investigated in the temperature range 204–304 K in CD_2Cl_2 . The aromatic section of ^1H NMR spectra clearly exhibits the passage from slow to fast exchange (see Figure 3) for all but the 6–6' proton pairs. The rate constants of exchange for complexes **2a–f** at different temperatures were determined by a full line shape analysis. The thermodynamic parameters of activation for the exchange process were derived from Eyring plots and are collected in Table 2. The ΔG^\ddagger_{298} values agree with those reported in the literature for similar processes¹³ and are not significantly affected by the nature of the counterion. The activation entropies are negative for all the complexes except **2f**. For complex **2f** ΔS^\ddagger is slightly positive. This means that $\text{B}(3,5\text{-(CF}_3)_2\text{C}_6\text{H}_3)_4^-$ in both the ground state and the transition state that attend to the dynamic process does not afford association with the cationic fragment. Complex **2a** is the only one where the entropic contribution ($T\Delta S^\ddagger_{298} = -32$ kJ/mol) is

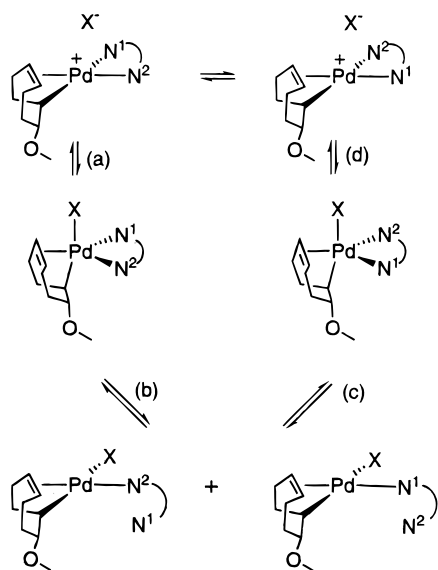
(10) Haigh, C. W.; Mallion, R. B. *Prog. NMR Spectrosc.* **1980**, *13*, 303–344.

(11) Strauss S. H. *Chem. Rev.* **1993**, *93*, 927–942.

(12) NOESY and HOESY NMR spectroscopies can detect only interionic dipolar interactions that are closer than 4.5–5 Å (ref 9) and are useful only when intimate ion-pairs are substantially present.

(13) (a) Gogol, A.; Ornebro, J.; Grennberg, H.; Bäckvall J.-E. *J. Am. Chem. Soc.* **1994**, *116*, 3631–3632. (b) Stockland, R. A. Jr.; Anderson, G. K. *Organometallics* **1998**, *17*, 4694–4699. (c) Groen, J. H.; Van Leeuwen, P. W. N. M.; Vrieze, K. *J. Chem. Soc., Dalton Trans.* **1998**, 113–117. (d) Gelling, A.; Orrell, K. G.; Osborne, A. G.; Sik, V. *J. Chem. Soc., Dalton Trans.* **1998**, 937–945.

Scheme 2



higher, in absolute value, than the enthalpic one ($\Delta H^\ddagger = 26$ kJ/mol). This is in agreement with the tendency of BPh_4^- to associate with the electrophilic fragment,¹⁴ which, in some cases, activates a phenyl group.

In the case of complex **2d**, the process that equilibrates the two pyridyl rings was investigated in the presence of excess amounts of free bipy (up to 1:4) and counterion (up to 1:8). The addition of free bipy increased the process rate, and there was also a slight increase in the process rate when an excess of counterion was added. This increase was less marked than that caused by the addition of free N,N-ligand and can be reasonably attributed to a further shift of the ion-pair dissociation equilibrium toward the intimate ion-pairs. The two experiments carried out in the presence of a 4- and 8-fold excess of counterion afforded the same rate constants, which indicates that, in both cases, the solution is made up of nearly 100% intimate ion-pairs.

The reaction mechanism that we consider more probable for the exchange of the two pyridyl rings in complexes **2a–e** involves (see Scheme 2) (a) the association of the counterion with the palladium, which leads to a five-coordinate intermediate, (b) the dissociation of an N-arm that can afford two different complexes where the bipy is η^1 -coordinated, (c) the re-entry of the free N-arm, and (d) the dissociation of the anion X^- . However, the rearrangement of the five-coordinated intermediate via Berry pseudorotation¹⁵ or "turnstile"¹⁶ mechanisms cannot be excluded.

The associative nature of the process is supported by the negative values of the entropy of activation. Furthermore, previous studies¹⁷ showed that a five-coordi-

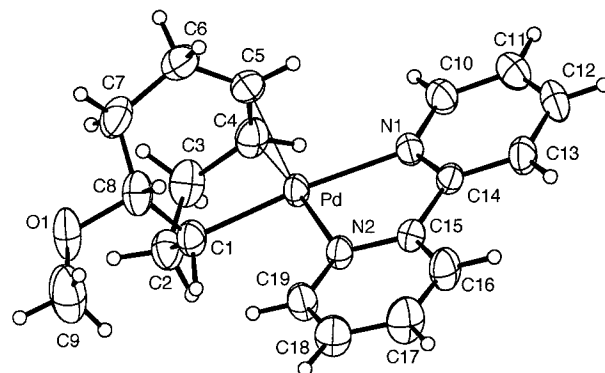


Figure 4. Molecular structure and atom-labeling scheme of the $[\text{Pd}(\eta^1, \eta^2\text{-C}_8\text{H}_{12}\text{OMe})\text{bipy}]^+$ cation. Thermal ellipsoids are drawn at the 40% probability level.

nate complex, analogous to that derived from the association of **2** with the counterion, can be isolated and characterized when $\text{X}^- = \text{Cl}^-$.

In the case of complex **2f**, the equilibrium of step (a) is shifted toward the free ions, as indicated by the high values of ΔH^\ddagger ($=61$ kJ/mol) and ΔS^\ddagger ($=13$ J/mol K); the mechanism could also be dissociative, involving a T-shaped 14-electron three-coordinate molecular fragment.¹⁸

The results of the experiments carried out in the presence of an excess of free bipy could also be explained with the proposed mechanism. In fact, free bipy can compete with X^- on attacking the apical position in (a). The second N-arm of bipy can substitute an N-arm of the coordinated bipy, giving an intermediate that is analogous to the one coming from process (b) where, instead of X, there is another η^1 -coordinated bipy. A $^{19}\text{F}\{^1\text{H}\}$ HOESY spectrum was recorded for complex **2d** at 217 K in the presence of an excess (2:1) of free bipy. Unfortunately, due to the exchange processes within the coordinated bipy and between the free and coordinated bipy, no useful information was obtained. The spectrum shows the same interionic contacts with the same intensities as that recorded without the excess of free bipy. There are also contacts with all the protons of the free bipy.

(d) Solid State: X-ray Structure of 2d. A perspective drawing of the molecule with the atom-numbering scheme is shown in Figure 4; a selection of bond lengths and angles is reported in Table 3.

The environment of the palladium atom is essentially square planar (Figure 4) with the bipy molecule acting as bidentate ligand (planar within $\pm 0.043(4)$ Å), and the organic octa-membered ring is linked through a σ -bonded carbon atom (C(1)) and a π -olefinic bond (C(4)–C(5)). The molecular structure of the cation shows an exo orientation of the methoxy group, which was also as detected in solution. Inspection of the data of Table 3 shows that the Pd–N(1) bond distance (2.154(3) Å) is about 0.05 Å longer than the Pd–N(2) one (2.105(3) Å), because of the influence exerted by the σ -bonded C(1) atom in the trans position. On the other hand, the Pd–

(14) Fachinetti, G.; Funaioli, T.; Zanazzi, P. F. *J. Chem. Soc., Chem. Commun.* **1988**, 1100–1101. Jordan, R. F. *Adv. Organomet. Chem.* **1991**, *32*, 325–387. Horton, A. D.; Frijns, J. H. G. *Angew. Chem., Int. Ed. Engl.* **1991**, *30*, 1152–1154. Bochmann, M.; Jaggar, A. J.; Nicholls, J. C. *Angew. Chem., Int. Ed. Engl.* **1990**, *29*, 780–782. Hlatky, G. G.; Turner, H. W.; Eckman, R. R. *J. Am. Chem. Soc.* **1989**, *111*, 2728–2729. Taube, R.; Krukowka, L. *J. Organomet. Chem.* **1988**, *347*, C9–C12. Turner, H. W.; European Patent Appl. 277004 (assigned to Exxon), 1988. Lin, Z.; Lo Marechall, J.-F.; Sabat, M.; Marks, T. J. *J. Am. Chem. Soc.* **1987**, *109*, 4127–4129. Jordan, R. F.; Bajgur, C. S.; Willett, R.; Scott, B. J. *Am. Chem. Soc.* **1986**, *108*, 7410–7411.

(15) Cesares, J. A.; Espinet, P. *Inorg. Chem.* **1997**, *36*, 5428.

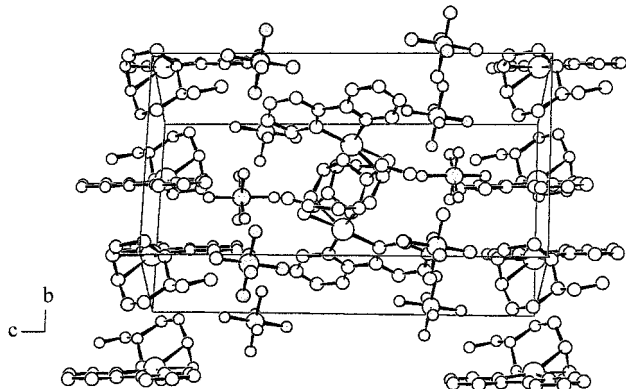
(16) Ugi, I.; Marquarding, D.; Klusacek, H.; Gillespie, P. *Acc. Chem. Res.* **1971**, *4*, 288.

(17) Albano, V. G.; Castellari, C.; Morelli, G.; Vitagliano, A. *Gazz. Chim. Ital.* **1989**, *119*, 235–239. For a review on five-coordinated alkene complexes of Pd(II) and Pt(II) see: Albano, V. G.; Natile, G.; Panunzi, A. *Coord. Chem. Rev.* **1994**, *133*, 67–114.

(18) Romeo, R.; Monsù Scolaro, L.; Nastasi, N.; Arena, G. *Inorg. Chem.* **1996**, *35*, 5087–5096, and references therein.

Table 3. Relevant Bond Lengths [Å] and Angles [deg] for 2d

Pd–C(1)	2.040(3)	Pd–C(5)	2.175(3)
Pd–N(1)	2.154(3)	Pd–C(4)	2.190(4)
Pd–N(2)	2.105(3)	C(5)–C(4)	1.367(6)
C(1)–Pd–N(1)	174.57(12)	N(2)–Pd–C(5)	150.18(14)
C(1)–Pd–N(2)	97.79(12)	N(2)–Pd–C(4)	173.28(13)
C(1)–Pd–C(4)	80.03(14)	C(5)–Pd–C(4)	36.5(2)
C(1)–Pd–C(5)	88.9(2)	C(8)–C(1)–Pd	110.1(3)
N(2)–Pd–N(1)	77.72(10)	C(2)–C(1)–Pd	109.5(2)
N(1)–Pd–C(4)	104.09(13)	C(4)–C(5)–Pd	72.3(2)
N(1)–Pd–C(5)	96.52(12)		

**Figure 5.** Crystal structure as viewed along the crystallographic axis *a*.

C(1) bond distance (2.040(3) Å) is comparable to those found for other sp^3 carbons which are trans to a bipy nitrogen atom (2.023(4) Å¹⁹ and 2.036(6) Å²⁰).

As far as the Pd–olefin interaction is concerned, the structural data for some cycloocta- and cyclononadienes show that the square-planar coordination of the metal is defined by the midpoint of the carbon–carbon bond.²¹ In the present compound, atoms C(1), C(4), N(1), and N(2) settle a plane with max deviations of $\pm 0.031(2)$ Å, and therefore the Pd–C(5) and Pd–C(4) distances are slightly different (Table 3). The C=C bond distance of 1.367(6) Å is longer than the mean value of 1.318 Å reported for a *cis*-C–CH=CH–C group²² and indicates a π -back-donation of the filled metal d orbitals to the empty π ligand. However the olefin carbons maintain their sp^2 character, as attested by the coplanarity of the C(3), C(4), C(5), and C(6) atoms, whose mean plane defines a dihedral angle of 77.48(16)° with the coordination plane.

(e) Solid versus Solution Interionic Structure.

An interesting feature of the crystal structure is the pairs of complexes arranged about the crystallographic symmetry centers, while the PF_6^- anions are located sideways running along the *b* axis (Figure 5). The shortest contacts between the fluorine and the complex hydrogen atoms are about 2.5 Å, and there is no preferential location of the anions with respect to the

(19) Markies, A. B.; Rietveld, M. H. P.; Boersma, J.; Spek, A. L.; van Koten, G. *J. Organomet. Chem.* **1992**, *424*, C12–C16.

(20) Byers, P. K.; Canty, A. J.; Skelton, B. W.; White, A. H. *J. Organomet. Chem.* **1987**, *336*, C55–C60.

(21) Retting, M. F.; Wing, R. M.; Wiger, G. R. *J. Am. Chem. Soc.* **1981**, *103*, 2980–2986.

(22) Allen, F. H.; Kennard, O.; Watson, D. G.; Brammer, L.; Orpen, A. G.; Taylor, R. Typical interatomic distances: organic compounds. In *International Tables for Crystallography*, Wilson, A. J. C., Ed.; Kluwer Academic Publishers: Dordrecht, Boston, London, 1992; Vol. C.

Table 4. CO/Styrene Copolymerization: Effect of bipy Added to the Reaction Mixture^a

run	[bipy]/[Pd] ^b	g CP ^c	g CP/g Pd	M_w (M_w/M_n) ^d
1	1	1.05 (g)	395	27200 (2.3)
2	1.25	0.89 (w)	335	23000 (2.3)
3	1.5	0.84 (y)	316	22000 (3.0)
4	2	0.75 (y)	281	20200 (2.3)

^a Catalyst precursor: $[Pd(\eta^1, \eta^2-C_8H_{12}OMe)bipy]^+PF_6^-$. Reaction conditions: $n_{Pd} = 2.5 \times 10^{-5}$ mol; styrene $V = 20$ mL; solvent CH_2Cl_2 $V = 20$ mL; $T = 30$ °C; $P_{CO} = 1$ atm; $t = 4$ h. ^b In runs 2–4 free bipy added at the reaction mixture. ^c Color of the copolymer: g = gray, w = white, y = yellow. ^d Determined by GPC vs polystyrene standards.

complex. Moreover, no interaction between the metal and the counterion is evidenced, which means that packing forces in the solid state are predominant over $Pd \cdots F$ interactions. The interionic structure in solution deduced from the ¹H–¹⁹F dipolar interactions is reported in Figure 2. It may be due (1) to two types of ion-pairs which have the counterion above or below the coordination plane and shifted toward the pyridine ring trans to the Pd–C single bond or (2) to several types of ion-pairs, with each one contributing one or two interionic contacts where the counterion is located sideways to the “Pd-moiety”, as in the solid state. We believe that hypothesis (1) is more probable because the packing forces are absent in solution and the “natural” position to maximize electrostatic interactions is either above or below the coordination plane.

CO/Styrene Copolymerization. The monochelated monocationic compounds **2**, tested in the CO/styrene copolymerization, yielded perfectly alternating polyketones, whose characterization (elemental analyses, IR, ¹H and ¹³C NMR spectra) is in agreement with the literature data.^{23,24} Some preliminary results have evidenced that these compounds are active catalyst precursors in nonalcoholic medium without any acid cocatalyst or any oxidant.⁶ Moreover, the 2,2'-bipyridine was the most active ligand tested.⁶

The copolymerization reactions were carried out in a thermostated glass reactor under a continuous flow of CO. When the hexafluorophosphate derivative was used as catalyst precursor, almost 400 g CP/g Pd (g CP/g Pd = grams of copolymer per gram of palladium) was obtained after 4 h; the CO/styrene polyketone has a molecular weight of 27200 amu (Table 4, run 1). However, the gray color of the copolymer indicates that the active species partially decomposed into palladium metal.

The catalytic system was optimized toward the stability of the active species by adding different amounts of free bipyridine to the reaction mixture. The addition of small amounts with respect to palladium decreased productivity of the system, which corresponded to a slight decrease in the molecular weight of the copolymers (Table 4, runs 2–4). It can be noted that as soon as a small amount of free bipy was added, the copolymer was white, indicating a negligible decomposition to metal; yellow copolymers were obtained when increased amounts of bipy were added. The filtered yellow poly-

(23) Milani, B.; Alessio, E.; Mestroni, G.; Sommazzi, A.; Garbassi, F.; Zangrando, E.; Bresciani-Pahor, N.; Randaccio, L. *J. Chem. Soc., Dalton Trans.* **1994**, 1903–1911.

(24) Barsacchi, M.; Consiglio, G.; Medici, L.; Petrucci, G.; Suter, U. *W. Angew. Chem., Int. Ed. Engl.*, **1991**, *30*, 989–991.

Table 5. CO/Styrene Copolymerization: Effect of the Anion^a

run ^b	X	g CP	g CP/g Pd	M _w (M _w /M _n) ^c
1	B(3,5-(CF ₃) ₂ C ₆ H ₃) ₄ ⁻	1.45 (lg) ^d	545	24000 (2.3)
2	SbF ₆ ⁻	1.14 (g)	429	27000 (2.3)
3	PF ₆ ⁻	1.05 (g)	395	27200 (2.3)
4	BF ₄ ⁻	0.74 (g)	278	26600 (2.2)
5	CF ₃ SO ₃ ⁻	0.20 (g)	75	9200 (1.5)
6	SbF ₆ ⁻	0.80 (y)	301	22600 (2.2)
7	PF ₆ ⁻	0.75 (y)	281	20200 (2.3)
8	B(3,5-(CF ₃) ₂ C ₆ H ₃) ₄ ⁻	0.72 (w)	271	18800 (2.6)
9	BF ₄ ⁻	0.69 (y)	259	20700 (2.2)
10	CF ₃ SO ₃ ⁻	0.18 (y)	68	9700 (1.6)

^a Catalyst precursor: [Pd(η¹,η²-C₈H₁₂OMe)bipy]⁺X⁻. Reaction conditions: n_{Pd} = 2.5 × 10⁻⁵ mol; styrene V = 20 mL; solvent CH₂Cl₂ V = 20 mL; T = 30 °C; P_{CO} = 1 atm; t = 4 h. ^b Runs 6–10 free bipy added: [bipy]/[Pd] = 2. ^c Determined by GPC vs polystyrene standards. ^d Color of the copolymer: lg = light gray.

ketones which were stirred in methanol, at room temperature, turned to gray after 30 s. This observation suggests that the polymeric chains are bonded to palladium and the treatment with methanol causes the alcoholysis of the Pd–C bond with the formation of palladium metal. A similar behavior has recently been reported for living CO/olefin alternating copolymerization promoted by [iodo(*endo*-6-phenyl-2-norbornene-*endo*-5σ,2π)(PPh₃)Pd(II)].²⁵

The effect of the anion was investigated in both the presence and absence of free bipy, added to the reaction mixture. In its absence productivity decreased from B(3,5-(CF₃)₂C₆H₃)₄⁻ to CF₃SO₃⁻, the complex with the B(3,5-(CF₃)₂C₆H₃)₄⁻ anion being the most active (Table 5, runs 1–5). The anion had no effect on the molecular weight except for the triflate derivative (Table 5, run 5), which is also much less active than the other complexes.

When the same analysis was repeated by adding free bipy in a 1:1 ratio with respect to palladium, the compound with the B(3,5-(CF₃)₂C₆H₃)₄⁻ anion had a productivity slightly lower than that of the SbF₆⁻ and PF₆⁻ derivatives. Due to the addition of the free bipy, the nature of the anion does not influence the catalytic activity of the system, with the exception of triflate (Table 5, runs 6–10). As expected, the polyketones obtained have very similar molecular weights. The complex with the BPh₄⁻ anion was completely inactive with the active species decomposing very quickly to metal either in the absence or presence of excess bipy. A similar behavior has been reported for the compound [Pd(bipy)₂](BPh₄)₂ when used as a catalyst precursor for the reductive carbonylation of nitroaromatic compounds into urethanes and was explained by assuming a phenyl group transfer from the anion to Pd(II).²⁶

On the basis of the interionic structure, evidenced in solution, the effect of the anion on the catalytic activity of the system, in the absence of added bipy, may be related to the strength of interionic interactions. Productivity increases as the interionic interactions decrease. It is the highest for the B(3,5-(CF₃)₂C₆H₃)₄⁻ derivative, which affords very little concentration of intimate ion-pairs. Indeed, the position of the anion

favors the dissociation of one N-arm of the bipy molecule and, therefore, the decomposition of the active species to metal.

In agreement with the above observation, when the copolymerization reactions were carried out in the presence of an excess of bipy with respect to palladium, the active species was stable and no significant effect of the anion was found.

Conclusions

We have shown that monochelated monocationic Pd(II) complexes of the type [Pd(η¹,η²-C₈H₁₂OMe)bipy]⁺X⁻ are among the most active catalysts for the CO/styrene copolymerization carried out at room temperature and atmospheric pressure. The polyketones formed under such mild conditions have some of the highest molecular weights. Their activity decreases as the counterion becomes more coordinating. Furthermore, if the copolymerizations are carried out in the presence of an excess of free bipy, the catalytic activity decreases and the effect of the counterion is flattened.

Using ¹H NOESY and ¹⁹F{¹H} HOESY NMR spectroscopies, we have directly localized the counterion in methylene chloride solution with respect to the “Pd-moiety”. Regardless of the type of counterion, it is located above or below the coordination plane shifted toward the bipy ring trans to the σ-bond of the η¹,η²-cyclooctenyl ligand. This position differs from that observed in the solid state for complex **2d**, where the packing forces between different “Pd-moieties” predominate over the Pd···F interionic interactions, and consequently, the counterion lies on the side of the coordination plane.

In solution all complexes show a dynamic process that exchanges the two pyridyl rings. A variable-temperature NMR investigation showed that this process is affected little by the nature of counterion, even if it is favored by more coordinating counterions. The activation entropies are negative for all but **2f** complexes, suggesting an associative mechanism for the process. An excess of free bipy accelerates the process. An excess of counterion slightly favors the process, but the effect is less marked and can be reasonably attributed to a shift of the ion-pair dissociation equilibrium toward the intimate ion-pairs.

Experimental Section

General Data. Reactions were carried out in a dried apparatus under a dry inert atmosphere of nitrogen using standard Schlenk techniques. Solvents were purified prior to use by conventional methods.²⁷ The methylene chloride (Baker) was used without further purification for the copolymerization reactions. Carbon monoxide (CP grade, 99.9%) was supplied by SIAD.

IR spectra were taken on a 1725 X FTIR Perkin-Elmer spectrophotometer. One- and two-dimensional ¹H, ¹³C, ¹⁹F, and ³¹P NMR spectra were measured on Bruker DPX 200 and DRX 400 spectrometers. Referencing is relative to TMS (¹H and ¹³C), CCl₃F (¹⁹F), and 85% H₃PO₄ (³¹P). NMR samples were prepared dissolving about 20 mg of compound in 0.5 mL of CD₂Cl₂. An appropriate quantity of NBu₄PF₆ was added for the experiments carried out for complex **2d** in the presence of an excess

(25) Safir, A. L.; Novak, B. M. *J. Am. Chem. Soc.* **1998**, *120*, 643–650.

(26) Bontempi, A.; Alessio, E.; Chanos, G.; Mestroni, G. *J. Mol. Catal.* **1987**, *42*, 67–80.

(27) Weissberger, A.; Proskauer, E. S. *Technique of Organic Chemistry*; Interscience: New York, 1955; Vol. VII.

of counterion. Two-dimensional ^1H NOESY and $^{19}\text{F}\{^1\text{H}\}$ HOESY spectra were obtained with a mixing time of 500–800 ms. Complex **1**²⁸ and $\text{B}(3,5\text{-}(\text{CF}_3)_2\text{C}_6\text{H}_3)_4^{29}$ were synthesized as previously reported in the literature.

Synthesis of Complexes 2a, 2d, and 2e. The ligand bipy (170 mg, 1.10 mmol) was added to a suspension of complex **1** (250 mg, 0.44 mmol) in methanol (10 mL) at room temperature. After that, the suspension became a yellow solution, the salt NaBPh_4 (**2a**), NH_4PF_6 (**2d**), or NaSbF_6 (**2e**) (1.80 mmol) previously dissolved in methanol was added, and a solid precipitated that was filtered off and washed with ethyl ether and dried under vacuum.

Complex 2a: white solid, yield 84%. Anal. Calcd (found) for $\text{C}_{43}\text{H}_{43}\text{N}_2\text{OBPD}$: C 71.54 (71.60); H 5.97 (6.03); N 3.89 (3.95). ^1H NMR (in CD_2Cl_2 , 217 K, J values in Hz): δ 8.52 (d, $^3J_{6,5} = 4.7$, 6'); 7.96 (td, $^3J_{4,5} = ^3J_{4,3} = 7.9$, $^4J_{4,6} = 1.2$, 4'); 7.87 (td, $^3J_{4,5} = ^3J_{4,3} = 7.9$, $^4J_{4,6} = 1.4$, 4); 7.72 (d, $^3J_{3,4} = 7.6$, 3'); 7.67 (d, $^3J_{3,4} = 8.1$, 3); 7.62 (d, $^3J_{6,5} \approx 5.4$, 6); 7.61 (dd, mixed with 6, 5'); 7.40 (dd, $^3J_{5,4} = 6.8$, $^3J_{5,6} = 5.4$, 5); 7.36 (m, *o*-H); 7.02 (t, $^3J_{m,o} = ^3J_{m,p} = 7.4$, *m*-H); 6.87 (t, $^3J_{p,m} = 7.2$, *p*-H); 5.79 (m, $^3J_{4,5} = 8.2$, 4'); 5.69 (dd, $^3J_{5,4} = 9.3$, $^4J_{5,3} = 3.5$, 5'); 3.66 (m, 8"); 3.41 (s, OMe); 2.92 (br, 1"); 2.82 (br d, $^2J_{6'a,6'b} = 17.6$, 6'a); 2.61 (m, 6'b); 2.36 (m, 2'a and 3'); 2.12 (m, 7"); 1.77 (m, 2'b).

Complex 2d: white solid, yield 84%. Anal. Calcd (found) for $\text{C}_{19}\text{H}_{23}\text{N}_2\text{OF}_6\text{PPd}$: C 41.68 (41.34); H 4.21 (4.48); N 5.13 (4.91). ^1H NMR (in CD_2Cl_2 , 217 K, J values in Hz): δ 8.60 (dd, $^3J_{6,5} = 5.8$, $^3J_{6,4} = 1.2$, 6'); 8.40 (dd, $^3J_{3,4} = 8.3$, $^3J_{3,5} = 1.3$, 3'); 8.32 (td, $^3J_{4,5} = ^3J_{4,3} = 8.0$, $^4J_{4,6} = 1.5$, 4'); 8.32 (d, $^3J_{3,4} = 8.2$, 3); 8.20 (td, $^3J_{4,5} = ^3J_{4,3} = 7.8$, $^4J_{4,6} = 1.6$, 4); 8.06 (dd, $^3J_{6,5} = 5.3$, $^4J_{6,4} = 1.2$, 6); 7.82 (ddd, $^3J_{5,4} = 7.5$, $^3J_{5,6} = 5.4$, $^4J_{5,3} = 1.3$, 5'); 7.72 (ddd, $^3J_{5,4} = 7.6$, $^3J_{5,6} = 5.3$, $^4J_{5,3} = 1.1$, 5); 6.09 (ddd, $^3J_{4,5} = 9.4$, $^3J_{4,3} = 6.9$, $^3J_{4,3} = 3.3$, 4'); 5.91 (ddd, $^3J_{5,4} = 9.2$, $^3J_{5,6} = 5.2$, $^3J_{5,6} = 2.4$, 5'); 3.67 (ddd, $^3J_{8,1} = 3.7$, $^3J_{8,7a} = 8.6$, $^3J_{8,7b} = 5.0$, 8"); 3.40 (s, OMe); 2.96 (ddd, $^3J_{1,2} = 3.6$, $^3J_{1,2'a} = 5.9$, $^3J_{1,2'b} = 2.3$, 1"); 2.87 (d, $^2J_{6'a,6'b} = 16.6$, 6'a); 2.67 (ddd, $^3J_{6,5} = 5.3$, 6'b); 2.38 (m, 2'a and 3'); 2.12 (m, 7"); 1.75 (m, 2'b). ^{13}C NMR (in CD_2Cl_2 , 217 K): δ 156.1 (s, 2' or 2); 153.1 (s, 2 or 2'); 148.7 (s, 6'); 148.0 (s, 6); 142.5 (s, 4'); 141.4 (s, 4); 128.4 (s, 5); 128.2 (s, 5'); 124.5 (s, 3'); 123.8 (s, 3); 107.5 (s, 5'); 106.6 (s, 4'); 82.5 (s, 8"); 56.9 (s, OMe); 53.5 (s, 1"); 33.8 (s, 2"); 30.7 (s, 7"); 29.5 (s, 6"); 26.5 (s, 3"). ^{31}P NMR (in CD_2Cl_2 , 304 K, J values in Hz): δ -141.3 (sept. $^1J_{\text{PF}} = 711.0$). ^{19}F NMR (in CD_2Cl_2 , 304 K, J values in Hz): δ -71.6 (d, $^1J_{\text{FP}} = 711.0$).

Complex 2e: yellow solid, yield 70%. Anal. Calcd (found) for $\text{C}_{19}\text{H}_{23}\text{N}_2\text{OF}_6\text{PdB}$: C 35.74 (36.02); H 3.61 (3.70); N 4.39 (4.30). ^1H NMR (in CD_2Cl_2 , 217 K, J values in Hz): δ 8.62 (dd, $^3J_{6,5} = 5.5$, $^3J_{6,4} = 1.5$, 6'); 8.39 (dd, $^3J_{3,4} = 8.2$, $^3J_{3,5} = 1.4$, 3'); 8.32 (td, $^3J_{4,5} = ^3J_{4,3} = 7.8$, $^4J_{4,6} = 1.5$, 4'); 8.31 (dd, $^3J_{3,4} = 8.1$, $^4J_{3,5} = 1.1$, 3); 8.20 (td, $^3J_{4,5} = ^3J_{4,3} = 7.7$, $^4J_{4,6} = 1.6$, 4); 8.07 (dd, $^3J_{6,5} = 5.3$, $^4J_{6,4} = 1.6$, 6); 7.83 (ddd, $^3J_{5,4} = 7.5$, $^3J_{5,6} = 5.5$, $^4J_{5,3} = 1.4$, 5'); 7.72 (ddd, $^3J_{5,4} = 7.6$, $^3J_{5,6} = 5.2$, $^4J_{5,3} = 1.2$, 5); 6.09 (m, $^3J_{4,5} = 9.5$, $^3J_{4,3} = 6.5$, 4"); 5.91 (ddd, $^3J_{5,4} = 9.3$, $^3J_{5,6} = 5.2$, $^3J_{5,6} = 1.7$, 5"); 3.68 (ddd, $^3J_{8,1} = 3.4$, $^3J_{8,7a} = 10.1$, $^3J_{8,7b} = 6.1$, 8"); 3.40 (s, OMe); 2.97 (m, 1"); 2.88 (d, $^2J_{6'a,6'b} = 18.4$, 6'a); 2.67 (m, $^3J_{6,5} = 5.6$, 6'b); 2.38 (m, 2'a and 3'); 2.14 (m, 7"); 1.75 (m, 2'b). ^{19}F NMR (in CD_2Cl_2 , 304 K, J values in Hz): δ -124.3 (superposition of a sextet due to $^{121}\text{SbF}_6^-$ and an octet due to $^{123}\text{SbF}_6^-$, $^1J_{\text{F}^{121}\text{Sb}} = 1946$ Hz, $^1J_{\text{F}^{123}\text{Sb}} = 1069$).

Synthesis of Complexes 2b and 2c. The procedure is similar to that reported above, but the precipitation following the addition of the salts (NaBF_4 or NaCF_3SO_3) is more difficult. For this reason the reactions were carried out in 10 mL of methanol and complexes **2b** and **2c** were precipitated by adding ethyl ether.

Complex 2b: white solid, yield 40%. Anal. Calcd (found) for $\text{C}_{20}\text{H}_{23}\text{N}_2\text{O}_4\text{F}_3\text{PdS}$: C 43.54 (43.23); H 4.17 (4.25); N 5.08

(5.25). ^1H NMR (in CD_2Cl_2 , 217 K, J values in Hz): δ 8.62 (d, $^3J_{6,5} = 4.5$, 6'); 8.52 (d, $^3J_{3,4} = 7.8$, 3'); 8.45 (d, $^3J_{3,4} = 8.2$, 3); 8.34 (td, $^3J_{4,5} = ^3J_{4,3} = 7.8$, $^4J_{4,6} = 1.4$, 4'); 8.21 (td, $^3J_{4,5} = ^3J_{4,3} = 7.9$, $^4J_{4,6} = 1.5$, 4); 8.11 (d, $^3J_{6,5} = 5.2$, 6); 7.83 (ddd, $^3J_{5,4} = 7.5$, $^3J_{5,6} = 5.5$, $^4J_{5,3} = 1.1$, 5'); 7.73 (dd, $^3J_{5,4} = 7.7$, $^3J_{5,6} = 5.3$, 5); 6.12 (m, $^3J_{4,5} = 9.0$, $^3J_{4,3} = 6.7$, 4'); 5.92 (ddd, $^3J_{5,4} = 9.3$, $^3J_{5,6} = 5.2$, $^3J_{5,6} = 1.9$, 5"); 3.68 (ddd, $^3J_{8,1} = 3.3$, $^3J_{8,7a} = 6.6$, $^3J_{8,7b} = 6.1$, 8"); 3.40 (s, OMe); 2.96 (m, 1"); 2.87 (d, $^2J_{6'a,6'b} = 18.2$, 6'a); 2.67 (m, 6'b); 2.39 (m, 2'a and 3"); 2.14 (m, 7"); 1.76 (m, 2'b). ^{19}F NMR (in CD_2Cl_2 , 304 K, J values in Hz): δ -79.3 (s).

Complex 2c: pale yellow solid, yield 83%. Anal. Calcd (found) for $\text{C}_{19}\text{H}_{23}\text{N}_2\text{OBF}_4\text{Pd}$: C 41.70 (42.10); H 4.70 (4.50); N 5.73 (5.55). ^1H NMR (in CD_2Cl_2 , 217 K, J values in Hz): δ 8.61 (dd, $^3J_{6,5} = 5.5$, $^3J_{6,4} = 1.6$, 6'); 8.46 (dd, $^3J_{3,4} = 7.7$, $^3J_{3,5} = 1.3$, 3'); 8.38 (dd, $^3J_{3,4} = 7.7$, $^4J_{3,5} = 1.2$, 3); 8.33 (td, $^3J_{4,5} = ^3J_{4,3} = 7.6$, $^4J_{4,6} = 1.6$, 4'); 8.21 (td, $^3J_{4,5} = ^3J_{4,3} = 7.7$, $^4J_{4,6} = 1.6$, 4); 8.09 (ddd, $^3J_{6,5} = 5.3$, $^4J_{6,4} = 1.7$, $^5J_{6,3} = 0.7$, 6); 7.82 (ddd, $^3J_{5,4} = 7.6$, $^3J_{5,6} = 5.5$, $^4J_{5,3} = 1.3$, 5'); 7.72 (ddd, $^3J_{5,4} = 7.6$, $^3J_{5,6} = 5.3$, $^4J_{5,3} = 1.2$, 5); 6.11 (ddd, $^3J_{4,5} = 9.4$, $^3J_{4,3} = 6.9$, $^3J_{4,3} = 3.3$, 4"); 5.91 (ddd, $^3J_{5,4} = 9.2$, $^3J_{5,6} = 5.2$, $^3J_{5,6} = 2.4$, 5"); 3.67 (ddd, $^3J_{8,1} = 3.6$, $^3J_{8,7a} = 5.1$, $^3J_{8,7b} = 6.1$, 8"); 3.40 (s, OMe); 2.97 (m, 1"); 2.86 (d, $^2J_{6'a,6'b} = 16.9$, 6'a); 2.69 (m, 6'b); 2.38 (m, 2'a and 3"); 2.12 (m, 7"); 1.75 (m, 2'b). ^{19}F NMR (in CD_2Cl_2 , 304 K, J values in Hz): δ -150.00 (br, $^{10}\text{BF}_4^-$); -150.06 (q, $^1J_{\text{FB}} = 1$, $^{11}\text{BF}_4^-$).

Synthesis of Complexes 2f. The ligand bipy (68 mg, 0.44 mmol) was added to a suspension of complex **1** (100 mg, 0.18 mmol) in methanol (8 mL) at room temperature. After the suspension became a yellow solution, an excess of the salt $\text{Na}^+(3,5\text{-}(\text{CF}_3)_2\text{C}_6\text{H}_3)_4\text{B}^-$, previously dissolved in methanol, was added and a solid precipitated that was washed with ethyl ether and dried under vacuum.

Complex 2f: white solid, yield 38%. Anal. Calcd (found) for $\text{C}_{51}\text{H}_{35}\text{N}_2\text{F}_{24}\text{BOPd}$: C 48.37 (48.55); H 2.77 (3.04); N 2.21 (2.43). ^1H NMR (in CD_2Cl_2 , 217 K, J values in Hz): δ 8.61 (d, $^3J_{6,5} = 5.5$, 6'); 8.19 (d, $^3J_{3,4} = 8.0$, 3'); 8.18 (td, $^3J_{4,5} = ^3J_{4,3} = 8.2$, $^4J_{4,6} = 1.3$, 4'); 8.12 (d, $^3J_{3,4} = 7.9$, 3); 8.07 (td, $^3J_{4,5} = ^3J_{4,3} = 7.5$, $^4J_{4,6} = 1.6$, 4); 7.97 (ddd, $^3J_{6,5} = 5.0$, 6); 7.76 (q, $^3J_{\text{H}11\text{B}} = 1.7$, *o*-H); 7.75 (ddd, partially buried under *o*-H, 5'); 7.61 (ddd, $^3J_{5,4} = 7.6$, $^3J_{5,6} = 5.2$, $^4J_{5,3} = 1.3$, 5); 7.57 (s, *p*-H); 6.05 (m, 4"); 5.87 (ddd, $^3J_{5,4} = 9.3$, $^3J_{5,6} = 5.3$, $^3J_{5,6} = 2.0$, 5"); 3.66 (ddd, $^3J_{8,1} = 3.4$, $^3J_{8,7a} = 5.1$, $^3J_{8,7b} = 6.1$, 8"); 3.39 (s, OMe); 2.97 (m, 1"); 2.85 (d, $^2J_{6'a,6'b} = 18.3$, 6'a); 2.68 (m, 6'b); 2.38 (m, 2'a and 3"); 2.13 (m, 7"); 1.76 (m, 2'b). ^{19}F NMR (in CD_2Cl_2 , 304 K, J values in Hz): δ -63.0 (s).

Variable-Temperature NMR Experiments. In a typical experiment, approximately 20 mg of complex was dissolved in 0.6 mL of CD_2Cl_2 . The ^1H NMR spectra were recorded over the temperature range 204–304 K. The spectra were simulated using the program DNMR3.³⁰ The exchange constants, obtained from the simulations, were used to determine ΔH^\ddagger , ΔS^\ddagger , and ΔG^\ddagger_{298} from the Eyring equation $k = (k_B/h)T \exp(-\Delta H^\ddagger/RT) \exp(\Delta S^\ddagger/R)$, where k_B is Boltzmann's constant, h is Planck's constant, and R is the ideal gas constant.

Catalysis. CO/Styrene Copolymerization Reactions. These reactions were carried out in a thermostated glass reactor (100 mL), equipped with a magnetic stirrer and a carbon monoxide gas line. After introducing the solvent, styrene, and catalyst precursor, carbon monoxide was continuously bubbled into the reaction mixture and heated to 30 °C. After 4 h the carbon monoxide flow was stopped and the reaction mixture was put into methanol (200 mL). The copolymer was filtered off, washed with methanol, and dried under vacuum.

Molecular Weight Measurement. The molecular weights (M_w) of the copolymers and the molecular weight distributions

(29) Brookhart, M.; Grant, B.; Volpe, A. F., Jr. *Organometallics* **1992**, *11*, 3920–3922.

(30) Kleier, D. A.; Binsch, G. DNMR3 Program 165, Quantum Chemistry Program Exchange, Indiana University, IN, 1970.

(28) Chatt, J.; Vallarino, L. M.; Venanzi, L. M. *J. Chem. Soc.* **1957**, 3413–3416.

(M_w/M_n) were determined by gel permeation chromatography versus polystyrene standards. The analysis were recorded on a Bruker HPLC (model LC-22) with an Alltech macrosphere GPC 60 E column and chloroform as solvent (flow rate 0.5 mL/min).

The CO/styrene copolymers were dissolved as follows: 3 mg of each sample was solubilized with 120 μ L of 1,1,1,3,3,3-hexafluoro-2-propanol (HFIP), and chloroform was then added up to 10 mL.

The statistical calculations were performed by using the Bruker Chromstar software program.

X-ray Analysis. X-ray Structure Determination of 2d.

$C_{19}H_{23}PdPF_6ON_2$, $M = 546.76$, monoclinic, space group $P2_1/n$ (alternative setting of no. 14), $a = 10.820(2)\text{\AA}$, $b = 10.161(1)\text{\AA}$, $c = 19.220(2)\text{\AA}$, $\beta = 95.89(6)^\circ$, $V = 2101.9(5)\text{\AA}^3$, $Z = 4$, $D_c = 1.728\text{ Mg/m}^3$, $\mu(\text{Mo K}\alpha) = 1.025\text{ mm}^{-1}$, $F(000) = 1096$. Diffraction measurements were carried out, at room temperature, on an Enraf-Nonius CAD4 diffractometer equipped with graphite monochromator and Mo K α radiation ($\lambda = 0.71073\text{\AA}$, θ range $2.07\text{--}26.97^\circ$, index ranges $-13 \leq h \leq 13$, $0 \leq k \leq 12$, $0 \leq l \leq 24$). A total of 4970 reflections were collected, of which 4565 were independent [$R(\text{int}) = 0.0282$]. The unit cell dimensions were refined by least-squares treatment of 25 reflections in the range θ $14\text{--}17^\circ$. The intensities of three standard reflections, measured at regular intervals throughout the data collection, showed no noticeable decay. All data were corrected for Lorentz-polarization effects and absorption (empirical ψ scan method), and the structure was solved by conventional Patterson³¹ and Fourier techniques and refined³² by the full-matrix anisotropic least-squares method on F^2 . The

final cycle of refinement, with the contribution of hydrogen atoms at fixed calculated positions, was based on 3486 observed reflections with $I > 2\sigma(I)$ and 272 parameters and converged with $R(F)$, $wR(F^2)$, and S (goodness-of-fit) to 0.0351, 0.0844, and 1.056, respectively. The largest residuals in the ΔF map were $+1.07$ and -0.95 e \AA^{-3} .

Acknowledgment. This work was supported by grants from the Ministero dell'Università e della Ricerca Scientifica e Tecnologica (MURST, Rome, Italy). Programma di Rilevante Interesse Nazionale, Cofinanziamento 1998–1999.

Supporting Information Available: Tables of crystal data and structure refinement (Table 1S), atomic coordinates and equivalent isotropic displacement parameters (Table 2S), bond lengths and angles (Table 3S), anisotropic displacement parameters (Table 4S), and hydrogen coordinates and isotropic displacement parameters (Table 5S) for **2d**. Kinetic rate constants for the process that equilibrates the two pyridine rings (Table 6S) for the complexes **2a–f**. This material is available free of charge via the Internet at <http://pubs.acs.org>. An X-ray crystallographic file is available in CIF format.

OM990372K

(31) Sheldrick, G. M. *Acta Crystallogr., Sect. A* **1990**, *A46*, 467–4730.

(32) Sheldrick, G. M. *SHELXL-97, Program for crystal structure refinement*; University of Göttingen: Germany, 1997.